ASCE

Unpacking Tornado Disasters: Illustrating Southeastern US Tornado Mobile and Manufactured Housing Problem Using March 3, 2019 Beauregard-Smith Station, Alabama, Tornado Event

Stephen M. Strader[1]; David B. Roueche, A.M.ASCE[2]; and Brett M. Davis, S.M.ASCE[3]

Abstract: This study illustrates and describes how Southeast US tornado disasters commonly unfold by examining the 2019 Beauregard-Smith Station, Alabama, tornado event from spatiotemporal and structural engineering standpoints. Findings indicate that although the meteorological forecasts leading up to the tornado event were accurate and timely, 23 individuals—19 in manufactured homes—still perished. All fatalities were primarily a result of the lack of positive ground anchoring on homes where individuals were killed. Altogether, the Beauregard-Smith Station, Alabama, tornado event resulted in a housing fatality rate seven times greater than the 2011 Joplin, Missouri, EF5 tornado at least in part due to a disproportionately larger number of manufactured homes exposed to violent tornado winds. Methods applied in this research should be utilized by future studies documenting tornadoes so that patterns in structural failure mechanisms and mortality can be determined. Integrated warning teams consisting of National Weather Service forecasters, emergency managers, media partners, etc. and members of the manufactured housing industry should work together using the results from this study to initiate a dialogue aimed at developing and improving tornado disaster mitigation, response, and recovery strategies. **DOI: 10.1061/(ASCE)NH.1527-6996.0000436.**

Introduction and Background

Tornadoes are one of the most costly and destructive hazards produced by severe convective storms. Six of the ten costliest tornadoes on record have occurred since 2011, resulting in over 300 fatalities and 3,300 injuries (NCEI 2019). Approximately 70 people per year (30-year mean) are killed by tornadoes, with most of these fatalities taking place in residential structures (Strader and Ashley 2018). High-impact tornado events are most common in the Southeast US, where tornado casualty rates are greatest due to a combination of factors such as a high percentage of housing stock that is mobile or manufactured homes (MHs), larger population and development density, elevated climatological tornado risk, and more physically and socially vulnerable residents compared to other tornado-prone regions in the US (e.g., Ashley 2007; Sutter and Simmons 2010; Ash 2017; Ashley and Strader 2016; Strader and Ashley 2018).

Tornado-MH Problem

There are two primary types of single-family residential structures, permanent homes (PHs) and MHs. Prior to 1976, any prefabricated (i.e., manufactured off-site) home was deemed a *mobile home*. In 1974, the US Congress passed the Housing Construction and Safety Standards Act, commonly called the Housing and Urban Development (HUD) code. The HUD code outlines and describes minimum construction guidelines or standards for newly built prefabricated homes. In 1994, HUD updated the code for MHs to significantly bolster design requirements in coastal areas—designated Wind Zones II and III—with success (FEMA 2007, 2013 cf. their Fig. G-1), but requirements for Wind Zone I—non-hurricane-prone regions of the US—remained largely unchanged. As such, any prefabricated home built after 1976 that follows the HUD code is referred to as a *manufactured home*. There is not a significant difference between pre- and post-1994 MHs homes with respect to design requirements in Wind Zone I. PHs are constructed in accordance with local building codes and designated as either a site-built or modular home. A modular home is prefabricated and assembled on site, while a site-built home is constructed from materials on location.

From a physical vulnerability and structural quality perspective, MH structures are expected to fail at wind loads less than 50% of those likely to destroy a PH (McDonald and Mehta 2004). As further evidence of this enhanced MH wind vulnerability, 54% of all housing-related tornado fatalities take place in MH structures even though only 6% of the entire US housing stock is made up of MHs (Strader and Ashley 2018). Further escalating housing-related tornado fatality odds, many states within the Southeast US region contain MH housing stock percentages that are more than double that of the national average (e.g., 13% in Alabama and 14% in Mississippi) according to census data. Simultaneously, a majority of MHs in the Southeast are located on isolated plots of land outside of city limits and not in MH communities or parks (Strader and Ashley 2018). This MH development pattern is unique to the Southeast, given that a majority of MHs in other regions such as the Midwest, Central Plains, Northeast, etc. are in urban- or suburban-density MH parks or communities.

[1]Assistant Professor, Dept. of Geography and the Environment, Villanova Univ., 800 E. Lancaster Ave., Mendel Hall G65F, Villanova, PA 19085 (corresponding author). ORCID: https://orcid.org/0000-0002-6472-3182. Email: stephen.strader@villanova.edu

[2]Assistant Professor, Dept. of Civil Engineering, Auburn Univ., Auburn, AL 36849. ORCID: https://orcid.org/0000-0002-4329-6759

[3]Graduate Research Assistant, Dept. of Civil Engineering, Auburn Univ., Auburn, AL 36849.

Note. This manuscript was submitted on March 30, 2020; approved on August 28, 2020; published online on December 15, 2020. Discussion period open until May 15, 2021; separate discussions must be submitted for individual papers. This paper is part of the ***Natural Hazards Review***, © ASCE, ISSN 1527-6988.

MH residents are also more likely to be socioeconomically vulnerable to tornado impacts because they regularly fall into one or several vulnerability-enhancing categories such as having a lower household income, relying on public assistance, and being disabled (Cutter et al. 2012; Ash 2017; Ash et al. 2020; Rumbach et al. 2020). Together, the greater number of less wind resistant housing structures, elevated socioeconomic vulnerability, and a larger percentage of MHs in rural or exurban areas in the Southeast elevates tornado impact and disaster potential within the region (Strader and Ashley 2018).

Postevent Tornado Damage Surveys

The first step in determining tornado impact severity and magnitude after an event is to conduct a rapid, postmortem analysis based on initial reports from sources such as first responders and affected populations. Following this initial assessment, an in-person, postevent damage survey is routinely conducted by a local National Weather Service (NWS) forecast office for the purpose of gathering information such as the tornado's wind speeds, path length, maximum path width, and damage magnitude (Marshall 2002; Prevatt et al. 2012b; Roueche and Prevatt 2013; Strader et al. 2014; Roueche et al. 2017). In high-impact events, it is also common for additional or complementary survey teams consisting of wind and structural engineers from academia, private industry, and government agencies to operate in parallel or assist the NWS with data collection (Prevatt et al. 2012a; Roueche and Prevatt 2013). These additional postevent damage assessments have proven useful for enhancing official NWS surveys by obtaining fine-scale details or information related to tornado damage indicators (DI), degree of damage (DOD), and tornadic wind field characteristics (Prevatt et al. 2012a; Roueche and Prevatt 2013; Burgess et al. 2014; Kuligowski et al. 2014; Lombardo et al. 2015; Egnew et al. 2018; Rhee and Lombardo 2018).

A principal objective of this study is to illustrate how Southeast US tornado disasters commonly unfold at the local scale and lead to fatalities due to the combination of a significant [Enhanced Fujita (EF) scale; EF2+] or violent (EF4+) tornado intersecting vulnerable MH residents. This study also demonstrates how high-resolution MH location data, fine-scale built environment, and land use-land cover (LULC) data can be combined with Doppler radar products in near-real time (i.e., as the tornado is still on the ground or within one hour after the tornado impacts a region) to estimate potential tornado impacts on the underlying landscape. Although prior research has illustrated that socioeconomic and demographic population characteristics play a role in tornado disaster severity, we do not assess or quantify these variables during the Beauregard-Smith Station, Alabama, tornado event because of the difficulty of acquiring fine-scale and accurate data linked to those that survived and/or were killed in the event. Nevertheless, the Beauregard-Smith Station, Alabama, tornado event is used as an exemplar for informing and applying near-real-time geospatial analyses within rapid, structure-by-structure tornado damage assessments to generate a more holistic, comprehensive, and thorough understanding of how tornadoes and elevated MH density in the Southeast US often lead to fatalities and disaster.

Data and Methodology

March 3, 2019 Severe Weather Conditions and Doppler Radar Data

To provide a detailed meteorological overview of the March 3, 2019 event, we first examined forecast discussions and products issued by the NWS and Storm Prediction Center (SPC) in the days and hours prior to the severe weather event. Additional tornado warning information was gathered from the Iowa Environmental Mesonet (IEM) storm warning verification tool to assess warning lead time for populations in Macon and Lee counties. Doppler radar base reflectivity, storm relative velocity, and correlation coefficient data from KMXX in southeastern Alabama were employed to illustrate the potential tornado damage path and intensity (NWS and KMXX Doppler Radar Site 2019). Complementary Multi-Radar/Multi-Sensor (MRMS) system rotation track data were also gathered to assist the raw Doppler radar data in determining a *potential* tornado damage area of interest (AOI) in near-real time (NSSL 2019).

Built Environment and LULC Data

A combination of fine-scale building footprint, land parcel, housing, critical infrastructure, and LULC data were employed to estimate potential tornado impacts in near-real time. Microsoft's US Building Footprints dataset was acquired to determine the number of structures (e.g., homes, public buildings, commercial buildings, barns, garages, sheds) that might have been damaged by the tornado (Microsoft US Building Footprints 2018). Additional built-environment entities such as homes, retail stores, restaurants, gas stations, office buildings, manufacturing/storage facilities, etc. were derived from county land-parcel data acquired prior to the event. Lastly, MH location data from Strader and Ashley (2018) were employed to provide a more complete and accurate representation of MH locations across Alabama.

In addition, Homeland Infrastructure Foundation-Level Data (HIFLD) was used in conjunction with land-parcel data to determine whether important or critical community, state, or federal structures were affected by the tornado (HIFLD 2020). The National Land Cover Database (NLCD) 2016 was also utilized to determine the types of LULC likely damaged in the tornado path (Wickham et al. 2014). The NLCD dataset comprises 15 LULC classifications, including four classes of developed land area (open, low-, medium-, and high-intensity development). A supplemental land use dataset [the Spatially Explicit Regional Growth Model (SERGoM)] was used in conjunction with the NLCD LULC data to estimate housing density within the potential tornado damage path (Theobald 2005). Housing unit density is broken down into four classes: urban [>9.9 homes per 0.01 km^2 (<0.1 ha per home)], suburban [1.24–9.8 homes per 0.01 km^2 (0.1–0.68 ha per home)], exurban [0.06–1.23 homes per 0.01 km^2 (0.68–16.18 ha per home)], and rural [<0.06 homes per 0.01 km^2 (>16.18 ha per home)].

Postevent Damage Survey Data Collected

Tornado damage information following the March 3, 2019 Beauregard-Smith Station tornado was collected using hands-on, door-to-door damage surveying techniques, drive-by damage assessments, targeted use of unmanned aerial systems (UAS), aerial imagery of the entire track captured from a low-flying aircraft, and synthesis of supplemental data sources (e.g., county property assessor information and preevent and postevent street view imagery hosted through Google Street View). Door-to-door damage observations were documented using the Fulcrum data collection platform from spatialnetworks.com, which uses a smartphone application to attach photographs and other media to a geolocated survey form. The survey forms applied in this study included a general building assessment sheet developed by the Structural Extreme Events Reconnaissance network (StEER; Kijewski-Correa et al. 2018) and a form specifically focused on MHs to allow for more precise details regarding anchorage, presence of corrosion, pier height variations, and

other critical construction and installation parameters to be collected in a standardized format.

Damage assessments documented the precise location, building attributes, structural load path, and observable damage, if present. Damage to buildings was assessed using the DODs in the EF scale and the StEER wind damage ratings, which categorize physical damage with an emphasis on resulting economic losses (Vickery et al. 2006). The assessments were further categorized by building type using the DIs of the EF scale. The commonly observed DIs (i.e., building types) were one- and two-family residences (DI2), single-wide MHs (SWMHs; DI3), and double-wide MHs (DWMHs; DI4), each of which have different DODs (i.e., progressive descriptions of damage unique to each DI) associated with them. To facilitate comparisons between these DIs in analyses, a degree of damage index (DODi) was developed and utilized to normalize the DODs for each DI. The DODi is defined as follows:

$$DODi(di, dod) = \frac{(WS_{di,dod} - WS_{di,DOD_1})}{(WS_{di,DOD_{max}} - WS_{di,DOD_1})} \quad (1)$$

where $WS_{di,dod}$ = expected wind speed for an observed DOD to a given DI; $WS_{di,DOD1}$ = expected wind speed for DOD1 (i.e., the threshold of visible damage for each DI); and $WS_{di,DOD_{max}}$ = expected wind speed associated with the highest DOD for the given DI. Thus, the DODi normalizes the damage in a 0–1 scale across all DIs, with 0 being the threshold of visible damage and 1 representing the highest damage state. For DIs 2, 3, and 4, DODi = 1 represents complete destruction with debris swept away from site for typical buildings. Further, the employed StEER wind damage ratings were modified to better separate economic destruction (i.e., structure is a total loss and must be replaced) from life-safety destruction (i.e., structure failed in such a way that life safety was put at risk). The original wind damage ratings are No Damage, Minor, Moderate, Severe, and Destruction. In the modified wind damage ratings, Destruction is split into two separate ratings, with Destruction (High Risk) representing any buildings in which all walls were collapsed—which also included lofting or rolling of MHs—and Destruction (Low Risk) representing structural failures which resulted in total loss economically but were a low life-safety risk due to walls and even portions of the roof still being intact to provide resident shelter.

Most buildings with considerable structural damage were investigated on-site between March 4 and March 13, 2019 by a team of two wind/structural engineers, while buildings in the outer regions of the tornado with minor or no damage were generally investigated via drive-by assessments and UAS/aerial imagery within the same time period, again by a team of two wind/structural engineers. Supplementary information such as photographs and narratives available from the NWS Damage Assessment Toolkit were used to augment the damage assessments when and where available. The tornado damage survey team placed an emphasis on collecting fine-scale and detailed information related to the structural performance of each home where a fatality occurred. Precise fatality locations were obtained using a variety of sources such as public media reports, social media posts related to the victims, and public tax assessor records.

In total, the postevent damage assessment documented the structural performance of 769 structures within the Alabama portion of the tornado damage path. Initial assessment targets were informed by the fine-scale MH dataset and geospatial assessments discussed in the previous sections. The ensuing assessments included 474 (62%) PHs, 229 (30%) MHs, and 64 (8%) other structures falling within a variety of classifications (including sheds and outbuildings), which included five churches and four buildings on the West Smith Station Elementary campus.

Overall, the study results are split into five primary sections (Fig. 1). Section "Meteorological Conditions, Forecast Performance, and Warning Lead Times" provides a summary and temporal perspective on the meteorological conditions, forecast performance, and tornado warning lead times prior to the Beauregard-Smith Station tornado. Section "Assessing Potential Impacts in Near-Real Time using Radar, Built Environment, and LULC Data Prior to the Rapid Tornado Damage Survey" outlines and describes geospatial assessments of potential tornado impacts on the underlying landscape in near-real time and immediately following the tornado event. The analyses conducted in that section were also designed to inform the rapid, in-person, postevent tornado damage survey conducted in the days and weeks following the tornado. Section "Rapid In-Person, Postevent Damage Assessment" provides an overview of the structural performance of buildings in the damage path using fine-scale tornado damage survey techniques. Lastly, the results in Section "Event Fatalities, Circumstances, and Structural Performance" concentrate on those locations, circumstances, damage findings, etc. where fatalities occurred.

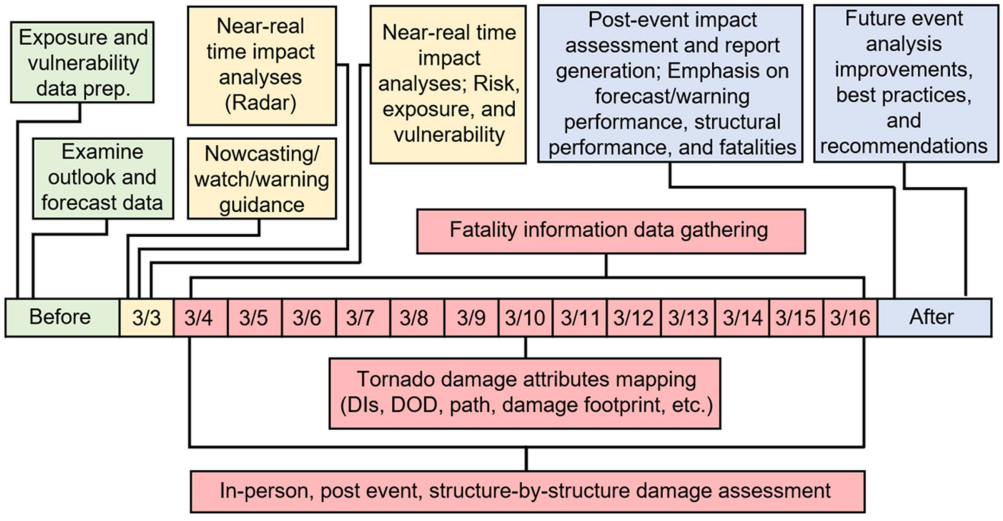

Fig. 1. Rapid tornado impact assessment timeline example using the Beauregard-Smith Station, Alabama, event.

Results

Meteorological Conditions, Forecast Performance, and Warning Lead Times

On March 1, 2019, the SPC released their Day 3 categorical and probabilistic severe weather outlooks, indicating a slight risk (15%) for the Southeast US [Fig. 2(a)]. While this initial forecast did mention the potential of a few tornadoes, the primary concern was storms that could produce straight-line winds, not rotating storms (e.g., supercells). Severe weather probabilities were amplified in the Day 2 SPC convective outlook released the day before the tornado event, increasing the probabilistic and categorical risk from 15% (slight) to 30% (enhanced) for areas of southeastern Alabama [Figs. 2(b and c)]. The primary forecast concern in the Day 2 outlook was the increasing likelihood of discrete supercells. For the Day 1 SPC outlook, severe weather probabilities were decreased from 30% to 10%. This reduction in severe weather potential was again due to concerns about a more dominant straight-line wind–producing storm mode (i.e., quasi-linear convective system) that would be less favorable for tornado production [Figs. 2(d and e)]. Similar to the Day 2 convective outlook, the Day 1 outlook noted that rotating storms and strong tornadoes would be possible where there would be a collocation of moderate instability (500–1,500 $J\,kg^{-1}$), high surface moisture [dew point temperatures of 15°C (60°F)], and strong low-level shear (50–70 kts) in the warm sector of the synoptic system.

At 15:59 UTC (9:59 AM CST) on March 3, 2019, the SPC issued their first mesoscale discussion (MD) for portions of southeastern Alabama [Fig. 2(f)]. This MD was released approximately two hours prior to the first tornado watch that covered the same region. The primary MD concern was the initial signs of discrete convection starting to develop in the warm sector where previous SPC outlooks had suggested some strong tornadoes could occur in southeastern Alabama. A second MD issued by the SPC at 18:02 UTC (12:02 PM CST) for portions of southeastern Alabama mentioned the amplifying likelihood for discrete supercell development and subsequent tornadoes over the next two hours [Fig. 2(g)]. Approximately an hour later, a third MD encompassing Macon and Lee counties was released based on radar imagery indicating a maturing supercell moving into an area that would be supportive of rotating thunderstorms and tornadoes [Fig. 2(h)]. In fact, the MD stated, "*Given the ample buoyancy and intense shear profile in place, it appears tornadogenesis will likely occur within the next 30–60 minutes with the possibility of a strong tornado occurring.*" After the Beauregard-Smith Station tornado formed, a final MD was issued at 20:19 UTC (2:19 PM CST) indicating that there was a high probability the outlined region could experience wind speeds of 125–175 mph [Fig. 2(i)].

The NWS Birmingham, Alabama weather forecast office issued the first tornado warning for the Beauregard-Smith Station, Alabama tornado at 19:19 UTC (1:19 PM CST). This warning yielded a 41-min lead time for those in far eastern Macon County where tornadogenesis eventually occurred. A second tornado warning was issued for Lee County at 19:58 UTC (1:58 PM CST) just prior to the tornadogenesis. The tornado warning for Lee County provided a lead time of approximately 5 min for the southwestern areas in Lee County and a 32-min lead time for eastern county portions. The location where most tornado fatalities occurred (i.e., Route 38 and Highway 51 in Lee County) received approximately 9 min of tornado lead time, which is less than the national average of approximately 15 min (Brooks and Correia 2018). Nevertheless, the SPC and NWS forecast was consistent and informative, providing Alabama residents with ample time to plan, prepare, and react to any severe weather threats. Yet, 23 individuals were killed, suggesting that other factors such as tornado intensity, population and built-environment exposure, building structural integrity, etc. played a more critical role during the event.

Assessing Potential Impacts in Near-Real Time Using Radar, Built Environment, and LULC Data Prior to the Rapid Tornado Damage Survey

Potential Impact Assessment: Doppler Radar Products

As the tornado event unfolded and immediately after the tornado was confirmed to be on the ground, we acquired a variety of raw and derived Doppler radar products covering Macon and Lee counties. There were five Doppler radar scans of the tornadic supercell made between tornadogenesis and prior to the tornado crossing the Alabama-Georgia state line [Fig. 3(a)]. The first Doppler radar base scan (0.5 degrees; lowest tilt) intersected the mesocyclone portion of the supercell in eastern Macon County at approximately 300 m (1,000 ft) above ground level (AGL). As the storm and tornado moved east-north easterly, a final base-level radar scan intersected the mesocyclone region of the supercell at 860 m (2,820 ft) AGL. The KMXX lowest-level radar tilt data were deemed sufficient for remotely determining the potential tornado damage path and assessing possible societal impacts prior to the in-person damage survey to be conducted on the following day because the radar was likely sampling the low-level mesocyclone portion of the storm responsible for the ongoing tornado.

The base reflectivity radar data illustrated a well-defined mesocyclone or hook echo on each scan from 20:01 UTC to 20:27 UTC. High base reflectivity returns of greater than 60 dBZ were also apparent in the hook echo region of the supercell at 20:07 UTC, highlighting a tornado debris signature [TDS; Fig. 3(a); Bodine et al. 2013; Van Den Broeke and Jauernic 2014]. Storm relative velocity data from the 20:07 UTC scan denoted a maximum rotational velocity of 57 kts [Fig. 3(b)]. This rotational velocity magnitude is consistent with prior research that has determined that rotational velocity values of 55–75 kts are commonly associated with significant tornadoes (Smith et al. 2015; Thompson et al. 2017; Gibbs and Bowers 2019). Correlation coefficient values less than 0.5 were also evident from 20:07 UTC to 20:27 UTC in the mesocyclone or updraft portion of the storm [Fig. 3(c)]. Radar scan tilts above base level illustrated correlation coefficient values consistent with debris being lofted by a significant tornado up to 5 km (16,400 ft; Kingfield and LaDue 2015). The MRMS rotation track denoted strong azimuthal shear values upward of 0.02 s^{-1} across Lee County [Fig. 3(d)]. Together, the base reflectivity, velocity, correlation coefficient, and rotation track data all indicated that it was likely that a significant or violent tornado traversed eastern Macon and southern Lee Counties from approximately 20:00 UTC to 20:30 UTC, causing substantial damage to the underlying landscape.

Potential Impact Assessment: Built Environment and LULC

A potential damage AOI based on the KMXX Doppler radar scans on March 3, 2019 from 20:01 UTC to 20:27 UTC was generated to assess potential built- and natural-environment impacts prior to the in-person damage assessment (Fig. 3). This AOI was intentionally designed to overestimate the tornado damage path so that it would represent a high-end impact estimate for the event. High-end impact estimates provide emergency managers and first responders with a worst-case scenario so that they can be best prepared to respond to any disaster situation. Based on the potential damage AOI, there were 2,791 buildings possibly damaged by the tornado. Approximately 67% of the buildings in the AOI were PHs or MHs, with 37% (1,020) being PHs. MHs represented 30%

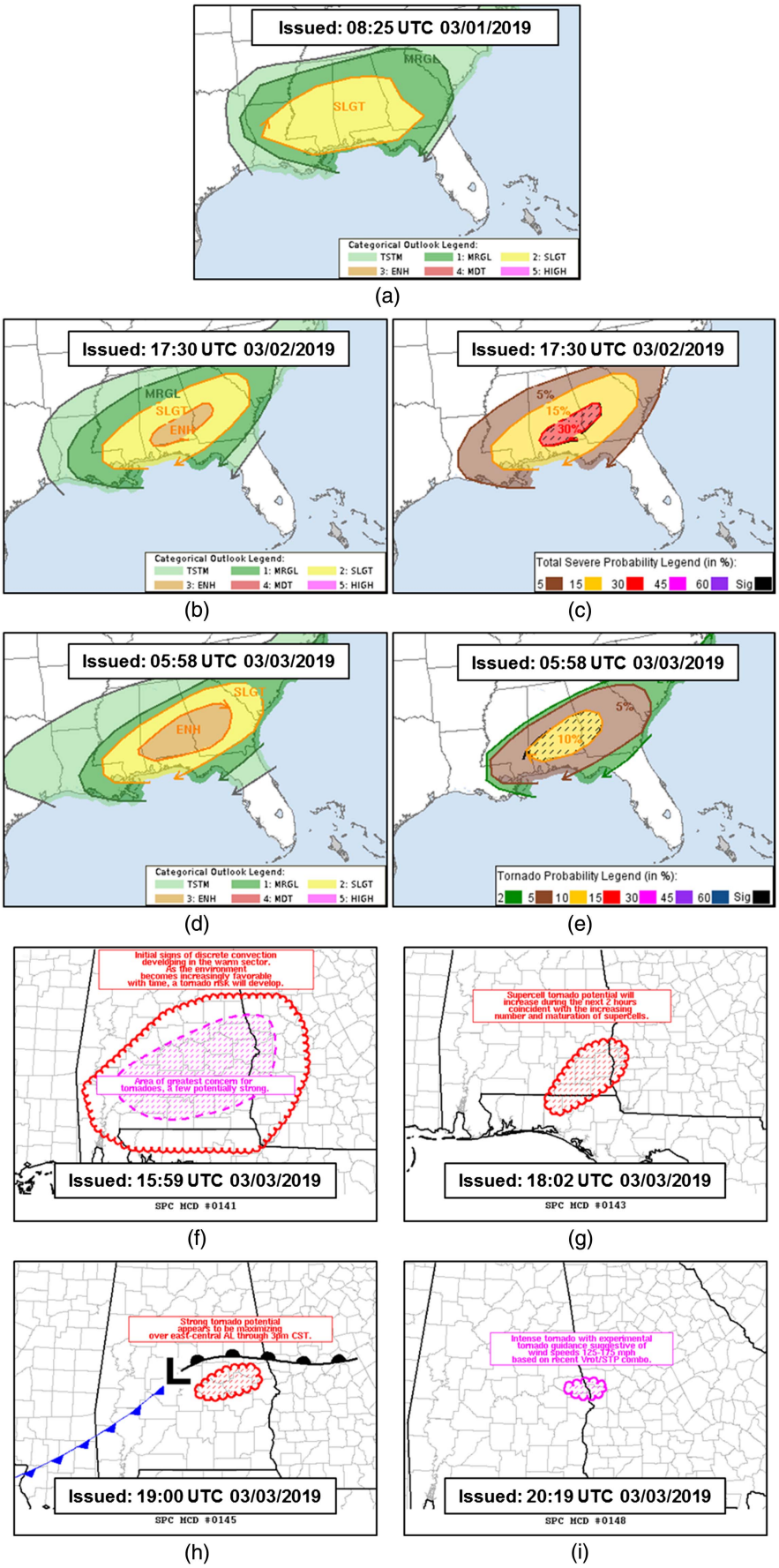

Fig. 2. (a, b, and d) Day 3–Day 1 SPC severe weather categorical outlooks; (c and e) tornado probabilities; and (f–i) MD for the March 3, 2019 Beauregard-Smith Station tornado. A dot represents the tornado path location in (a)–(e) and a line signifies the approximate location of the tornado path in (f)–(i).

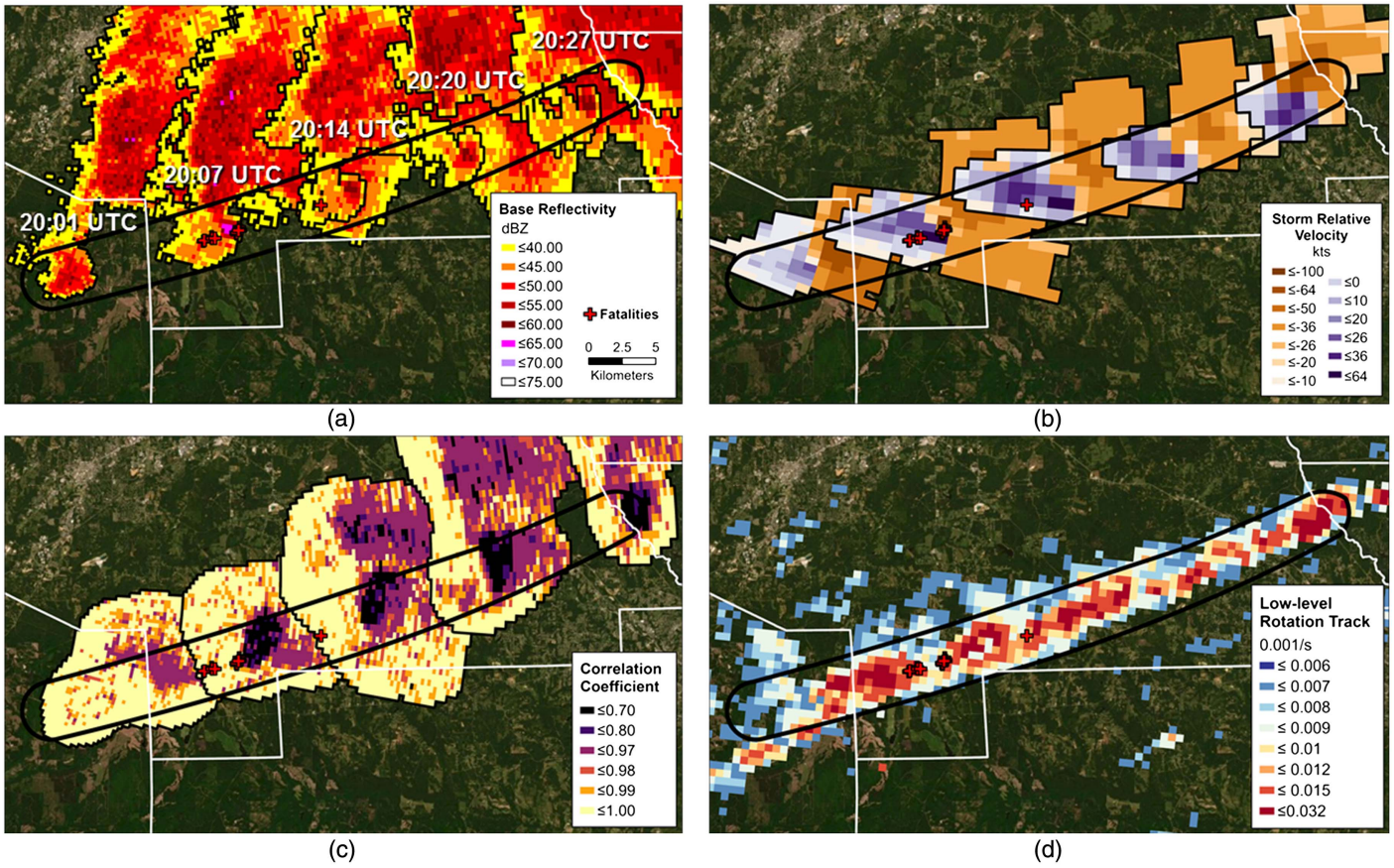

Fig. 3. KMXX raw and derived radar data from 20:01 UTC to 20:27 UTC: (a) base (0.5°; lowest tilt level) reflectivity (dBZ); (b) base storm relative velocity (kts); (c) correlation coefficient scan where a TDS was visually best evident; and (d) low-level rotation track (60 min., 0–2 km maximum azimuthal shear) from the MRMS project. Fatality locations are represented by crosses and the potential tornado damage AOI is outlined by the polygon.

(852) of all AOI building footprints and made up nearly 45% of all homes. This percentage of MH housing types is nearly 3.6 times greater than the Alabama state percentage of MH housing stock (13%; Census 2020). There were also six MH parks or communities in the potential damage AOI, with each of them containing less than 50 MH individual units. In addition to homes, there were approximately 44 other buildings within the AOI as well. These 44 buildings included churches, retail stores, gas stations or convenience stores, warehouses or manufacturing businesses, fire stations or emergency medical services, and an elementary/secondary school. Aside from buildings, there were 133 different roads, two high-tension power line regions, and a cell phone tower within the AOI. However, potential impact analyses also denoted that buildings such as federal, state, or local buildings; hospitals; university/college-related properties; etc. were not exposed to tornadic winds and subsequently damaged.

An estimated 84.1 km^2 (60%) of the AOI was estimated to be forested LULC, with evergreen forests representing the largest percentage of forested area at 23.3%. An additional 47.8 km^2 (34%) of the potential tornado damage AOI comprised natural and agricultural lands. Only 8.4 km^2 (6%) of the AOI region was considered developed LULC, with most (5.1 km^2) of the development being classified as open development (i.e., less than 20% impervious surfaces, with development being situated within mostly open areas and mixed vegetation). The SERGoM housing unit densities support this development character given that 96.3% of the potentially affected landscape was considered rural or exurban land use density. A majority 60% of the area underneath the AOI was considered exurban density. Only 1.1% of the exposed landscape was suburban or urban. Overall, the LULC and developed/housing unit density analyses indicate that the tornado may have crossed a largely undeveloped landscape where most homes in the region were in exurban density.

Rapid In-Person, Postevent Damage Assessment

The Beauregard-Smith Station tornado was rated an EF4 with an estimated maximum wind speed of 170 mph (NWS and BMX 2019). Tornadogenesis occurred at 20:00 UTC (2:00 PM CST) near Society Hill, Alabama, and continued east-northeast at approximately 60 mph. The tornado path length in Alabama was 44 km (27 mi) with a maximum path width of 1.5 km (1 mi). The tornado crossed the Alabama-Georgia state line at 20:29 UTC (2:29 p.m. CST) near Smith Station, Alabama. Overall, the tornado resulted in 23 fatalities and over 90 injuries, with most injuries occurring in the corridor from Lee Road 36 to Lee Road 38 in Lee County (Fig. 4). The locations of the fatalities and injuries aligned with the areas in which the most significant damage occurred, which was primarily in the first 20 km (12 mi) following tornadogenesis. The observed damage and MRMS data indicate that the tornado decreased in intensity as it moved toward Smith Station and across the Alabama-Georgia border. The rapid postevent assessment

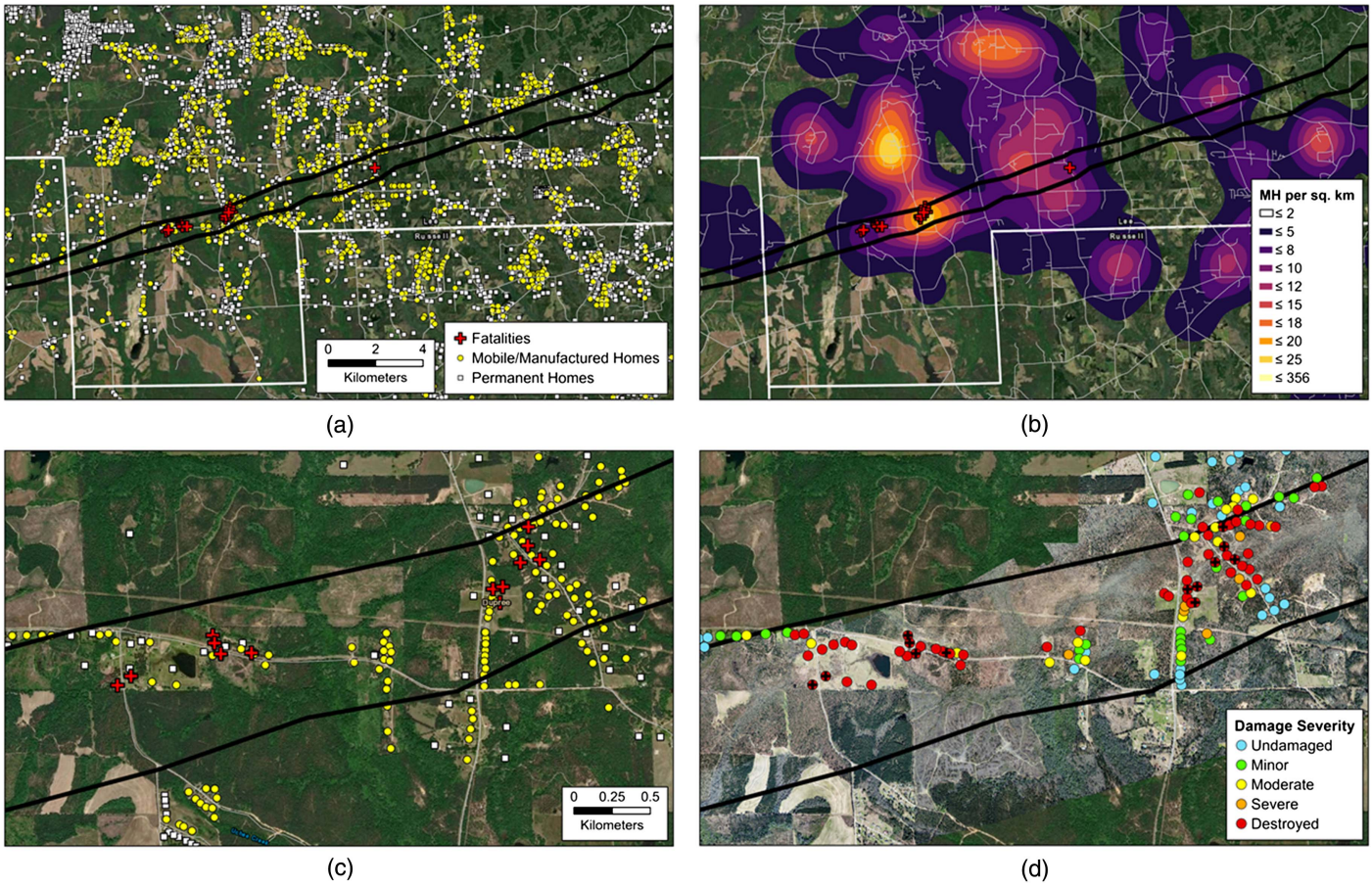

Fig. 4. Beauregard-Smith Station, Alabama, surveyed NWS tornado damage path (outlined polygon): (a) MH, PH, and fatality locations (cross); (b) MH density (MHs per km^2); (c) zoomed-in area of Route 36 to Route 38 in the Lee County, Alabama, region where most fatalities occurred; and (d) damage severity based on the postevent damage assessment.

identified a spectrum of performance across the various building typologies, primarily single-family homes (both PHs and MHs). A total of 380 buildings and other structures experienced visible exterior damage out of the 769 that could reasonably be assumed to have been affected by the tornado. The count of damaged buildings included 174 PHs (site-built or modular); 49 SWMHs; 105 DWMHs; 40 barns, sheds or similar buildings; and 12 nonresidential buildings. MHs comprised 47% of all residential structures that received visible exterior damage. SWMHs and DWMHs represented 15% and 32% of all homes damaged in the tornado, respectively. Nearly 70% of the MHs affected by the tornado were DWMHs as well. Together, these findings indicate that a disproportionately large percentage of MHs were exposed to the tornadic winds compared to the surrounding region (i.e., only 13% of the entire Alabama housing stock is made up of MHs).

The average (mean) year of construction for all buildings with visible damage was 1986, with means of 1984, 1994, and 1994, respectively for PHs, SWMHs, and DWMHs. The on-site, postevent tornado damage investigation found that construction quality within the path was generally poor to average, with no evidence of enhanced wind-resistance construction (e.g., metal strap roof-to-wall connections, oversized anchor bolt washers, structural wall sheathing throughout) in the vast majority of affected buildings. Specific to MHs, the investigation noted the common use of pan anchorage systems in lieu of traditional tie-down straps and ground anchors in newer MHs. These pan systems consisted of diagonal struts that transferred lateral loads to a metal pan that rests on the ground. The weight of the home is relied upon to both resist all uplift forces and provide sufficient gravity loads to create the static friction between the pan and the soil necessary to resist design lateral loads.

Wind performance for all buildings was primarily a function of the distance along the length of the tornado damage path and the distance from the centerline of the tornado [as estimated by the NWS (NWS and BMX 2019) damage path, approximate center of heaviest damage, and building typology (Fig. 5)]. Observations indicated that the robustness of the foundation or anchorage system played a significant role in determining a building's wind performance and/or damage severity within the tornado path. Although building orientation was a factor for all building types, the damage survey indicated that it was most important for MHs (Roueche et al. 2019). Significant damage to nonresidential structures was limited to older commercial and religious facilities with light-frame wood or unreinforced masonry structural systems. The most severe damage to nonresidential buildings was experienced by a small, unreinforced masonry church located near the beginning of the tornado path that was destroyed. No nonresidential structures were located within the path of the tornado when its intensity was the highest, near Highway 51 and Lee Road 38. Nonresidential structures were more common in and around Smith's Station, where the intensity of the tornado was reduced, and damage was very minor outside of a car dealership and restaurant. Both the car dealership and restaurant were older (pre-2000), light-frame buildings that experienced loss of the structural roof system. The only school affected within the

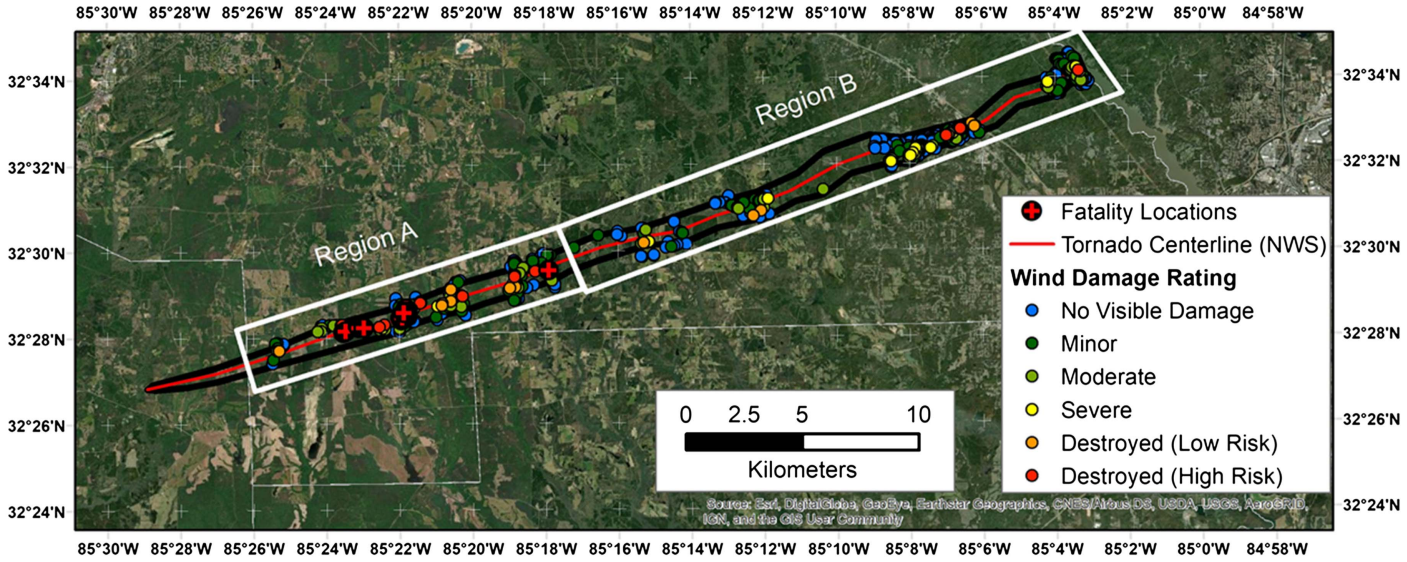

(a)

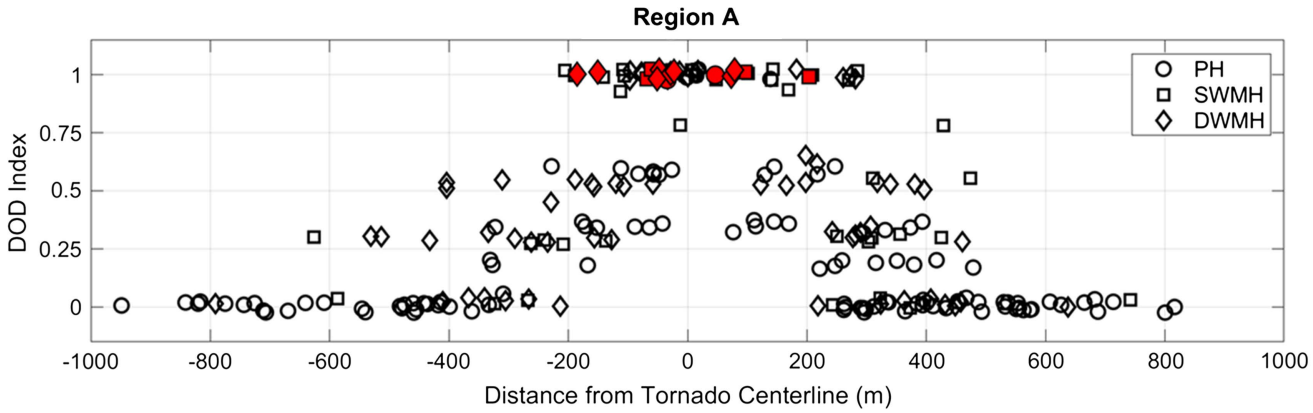

(b)

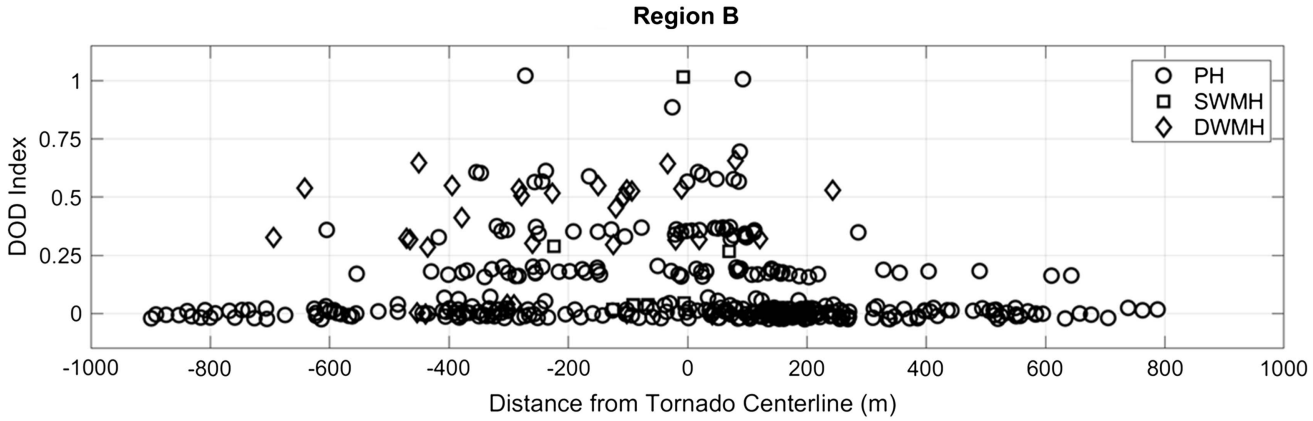

(c)

Fig. 5. Wind damage assessments for all structures in the tornado path: (a) spatial overview of entire tornado path using categorical damage ratings (base map by "World Imagery" Esri, Maxar, Earthstar Geographics, CNES/Airbus DS, USDA FSA, USGS, Aerogrid, IGN, IGP, and the GIS User Community); (b and c) DODi for SWMHs, DWMHs, and PHs in Regions A and B of the tornado with respect to the center of the tornado. Lines indicate average DODi over 200-m-wide bins. Negative distances indicate homes located on the north side of the centerline. Jitter has been added to the y-coordinates to facilitate better visualization. Filled markers in (b) and (c) indicate fatality locations. (d) Box plot indicating the median, 25th, and 75th percentiles of DODi for all PHs, SWMHs, and DWMHs in Regions A and B.

tornado path was the West Smith Station Elementary School, which experienced minor cladding damage, the collapse of a few exterior covered walkway structures, and the loss of some rooftop HVAC equipment. The tornado also induced the collapse of a cellular tower in Smith Station near US 280.

Of the 380 structures affected by the tornado, 328 were single-family homes (DIs 2, 3, and 4 in the EF scale). To better assess tornado impact severity to these structures, the tornado damage path was split into two primary geographic components, Region A and Region B (Fig. 5). The tornado path was split into these two regions based on damage severity and potential changes in tornado intensity as discussed previously. Damage was more severe within the first 20 km (12 mi) of the tornado path (designated Region A) than in the remainder of the path (designated Region B). Within Region A, complete structural failure in both PHs and MHs was most common within an approximately 250-m buffer on each side of the tornado centerline. Within this region, and in general across the entire tornado width in Region A, SWMHs sustained the highest damage on average, with PHs sustaining the lowest damage on average [Figs. 5(b and d)]. In Region B, extending from the edge of Region A to the Alabama-Georgia border, complete structural failure rarely occurred, despite similar building typologies, indicating the reduction in tornado intensity [Figs. 5(c and d)]. In both regions, SWMHs were the most likely to exhibit complete or catastrophic failure (Fig. 6), with 54% in Region A and 13% in Region B exhibiting damage with a high risk to life safety. This corresponded to 22 of the 41 damaged SWMHs in Region A, and one of the eight damaged in Region B, that experienced DOD6 or higher (i.e., the unit rolled, lofted, and/or experienced the destruction of the roof and all walls). DWMHs and PHs demonstrated better performance, with 29% (20 out of 70) of DWMHs and 16% (8 out of 50) of PHs with failures deemed high risk to life safety in Region A, and 0% (0 out of 35) and 2% (2 out of 124), respectively, in Region B. The two high-risk PH failures in Region B occurred in a section of poorly constructed, low-income homes in Smith Station.

The *key failure mechanism* that led to the destruction of several PHs and many MHs *was the lack of any positive anchorage to the ground*. Many PHs were simply resting on unreinforced masonry stem walls that offered no resistance to the uplift forces induced by a tornado, a weakness recognized in past studies also (e.g., Marshall 1993; Prevatt et al. 2012a). Where PHs were constructed on concrete slabs, with anchor bolts to the slab through the sill plates, at a

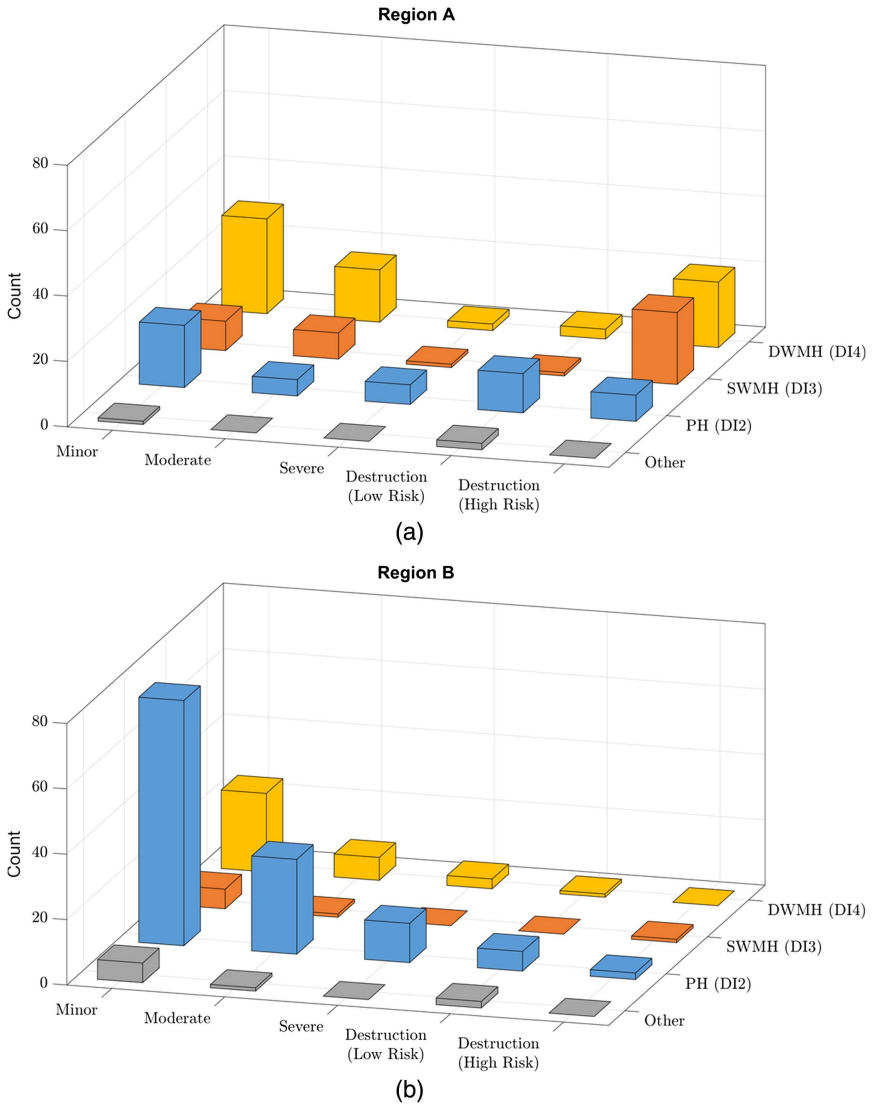

Fig. 6. Wind damage states of the affected buildings in (a) Region A; and (b) Region B using Vickery et al. (2006) but modified to separate economic destruction from destruction posing a high risk to life safety.

Nat. Hazards Rev., 2021, 22(1): 04020060

Fig. 7. Common anchorage problems encountered in the Beauregard, Alabama, tornado included (a and b) frequent use of pan-style alternative anchorage systems, which provide no uplift resistance; and (c) corrosion of diagonal ties and ground anchors. The plot (b) illustrates an overturned MH with a pan anchorage system. (Images by David B. Roueche and Brett M. Davis.)

minimum some walls were always left standing even with complete destruction of surrounding buildings. In MHs, previous studies have linked destruction with the lack of anchorage altogether (e.g., Kensler 1985; Sparks 1985), but in this study, all observed MHs appeared to have some anchorage/stabilizing system present at the time of tornado impact. However, the use of alternative pan anchorage systems, which rely upon the self-weight of the structure to resist any uplift forces, and the frequent corrosion of ground anchors and diagonal straps where used, compromised the wind resistance of these homes, potentially allowing catastrophic failures to occur at relatively low wind speeds (Fig. 7). For example, in several cases, the debris from a MH revealed that the home failed due to the radial inflow of the oncoming tornado, pulling the structure toward the tornado as it was destroyed. This complete destruction therefore occurred prior to when the tornado's most intense winds could impact the MH.

A considerable trend in the MH failures was the overall lack of an optimum damage progression. While damage generally initiated with loss of roof cover and cladding elements, very rarely was the loss of roof sheathing or roof structure observed with the anchorage system intact. The four primary mechanisms of structural failures observed in MHs consisted of the following: (1) separation at the marriage line (DWMHs only), (2) roof-to-wall connections, (3) wall-to-floor connections, and (4) failure of the anchorage system, resulting in either sliding, overturning, or lofting (Fig. 8). Of these potential mechanisms, the anchorage system was nearly universally the first element of the structural load path to fail during the tornado, compromising the entire structure and the safety of the occupants. This lack of safe failures in both SWMHs and DWMHs relative to PHs is exemplified in Fig. 6. Specifically, 12 of the 20 destroyed PHs in Region A were deemed low-risk failures in that at the very least some walls were left standing although the home was a total loss. In contrast, only 1 of the 23 destroyed SWMHs and 3 of the 23 destroyed DWMHs could be considered low-risk failures. Conversely, the remaining 19 MHs were destroyed with nothing left in their original locations as determined by the combination of the debris swaths, MH location data, and local parcel or tax records. The implications of this finding within the context of the fatalities that occurred are discussed later in this article.

Potential Tornado Damage AOI and Actual Postevent Damage Survey Impact Differences

As illustrated in the prior section, there were some differences between the real-time estimated tornado impact and postevent damage assessments. To determine the actual number of structures, facilities of interest, LULC percentages, etc. affected by the Beauregard-Smith Station tornado, a combination of the postevent tornado damage assessment and the NWS postevent surveyed tornado damage polygon was used. Given the coarse spatial resolution of the KMXX Doppler radar data, the potential tornado damage AOI overestimated the total impact on the underlying landscape. This finding was expected given that the AOI represented a potential damage area of 140 km^2 compared to an actual damage path area of approximately 40 km^2 based on the NWS-surveyed damage path. The larger potential tornado AOI compared to the actual damage path meant that some of the structures thought to be exposed in the tornado were not damaged. For example, none of the six MH parks, EMS/fire stations, manufacturing/warehouses, or office buildings sustained any visible tornado damage based on the postevent

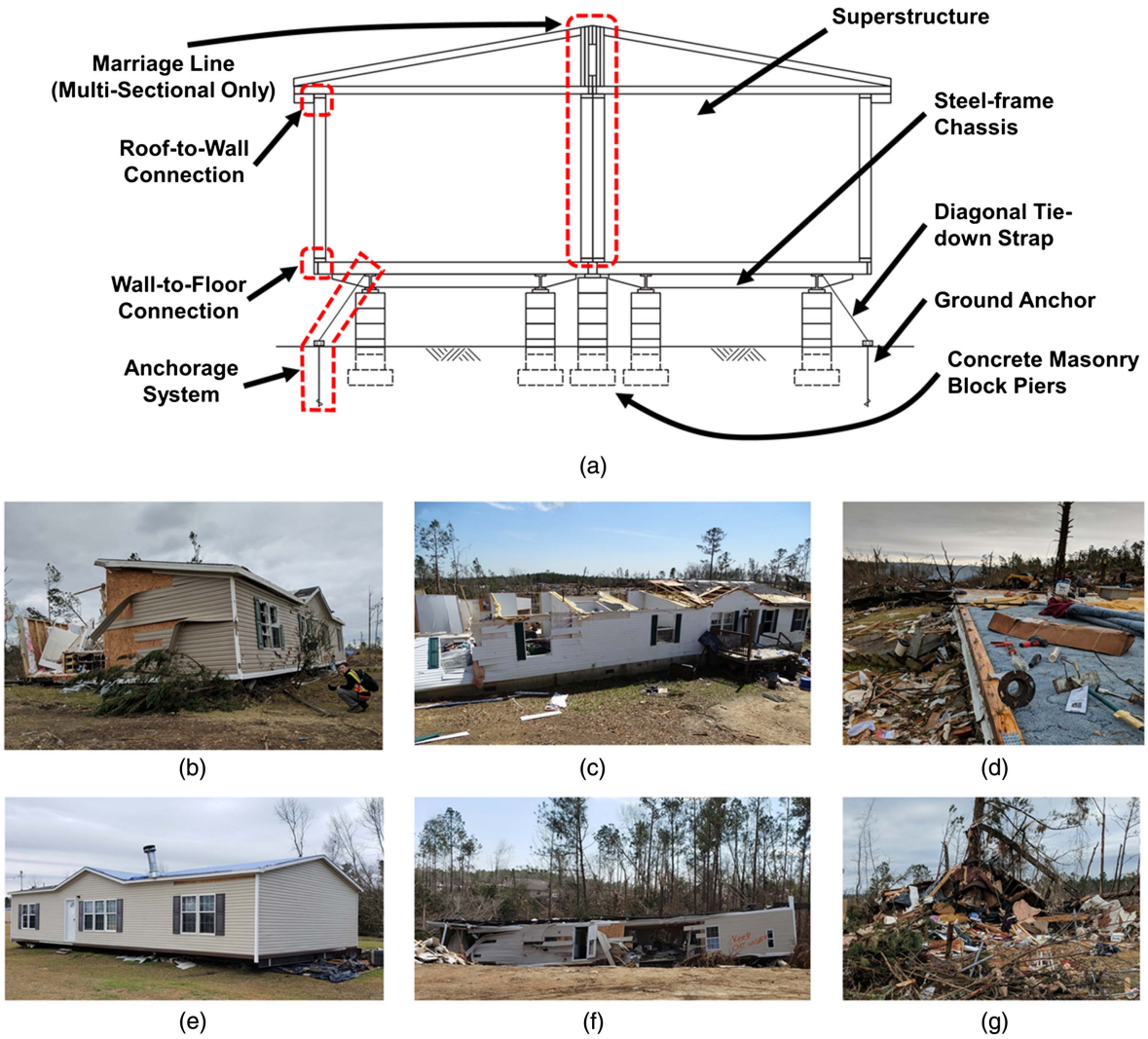

Fig. 8. (a) DWMH construction diagram with critical components and their locations labeled. Thick dashed lines highlight those areas where common failure mechanisms occur during tornado events and relate to the damage survey photos [(b)–(g)]. Failure mechanisms in MHs included (b) separation at the marriage line in DWMH; (c) roof-to-wall connection failures; (d) wall-to-floor connection failures; and (e and f) failures of the anchorage system, specifically (e) sliding; (f) overturning/rolling; and (g) lofting. (Images by David B. Roueche and Brett M. Davis.)

damage assessment. Although 12 churches were thought to be potentially struck by the tornado, only one received damage near the beginning of the tornado damage path.

Nevertheless, the near-real-time estimates of tornado damage using the AOI performed reasonably well. Doppler radar raw and derived products indicated that there was indeed a significant-to-violent tornado on the ground in southern Lee County, while the housing data suggested that a large number of MHs were potentially in the violent tornado's path. Further, LULC data illustrated that most of the MHs were not in MH communities, but rather in exurban or rural land use densities. The restaurant, car dealership, elementary school, and cell phone tower were all expected to have sustained damage based on the near-real-time assessment and did so based on the postevent damage survey.

In general, the near-real time provided immediate insight on potential tornado intensity and impacts. This type of analysis not only helped determine the severity of tornado impacts in real time but also provided much needed information for subsequent in-person, postevent assessments conducted in the days and weeks after. Not only will similar analyses be conducted for future potential high-impact tornado events, but additional modeling and analysis techniques will be added to the methodology so that damage estimation techniques can be improved. The ultimate goal of future work using this technique should be to provide a tool and methodology for NWS forecasters, emergency managers, first responders, and critical personnel to better estimate potential real-time tornado impacts on vulnerable populations.

Event Fatalities, Circumstances, and Structural Performance

In all, 19 of the 23 (82.6%) Beauregard-Smith Station tornado fatalities transpired in MHs (Roueche et al. 2019), and all fatalities occurred in homes that the posttornado event survey identified as high-risk failures. Fatalities occurred in 2 of the 8 PHs, 4 of the 23 SWMHs, and 8 of the 23 DWMHs that were deemed high-risk failures. Anchorage systems in these MHs were observed to be either pan systems or tie-down straps and ground anchors, but the precise details for each home's anchorage (e.g., number of anchors and connection details) could not always be discerned due to shifting or removal of the debris by first responders. Both PHs where victims were killed were wood-frame homes constructed atop

Table 1. Number of homes damaged, high-risk damaged homes, fatalities, and homes with fatalities for PHs, MHs (all types), DWMHs, SWMHs, and all home types. Fatality rates (fatalities per 100 damaged homes) for all damaged homes and all homes with high-risk damage are also calculated for the 2019 Beauregard-Smith Station, Alabama, tornado

Home type	Homes damaged	Homes with high-risk damage	Fatalities	Homes with fatalities	Fatality rate (per 100 damaged homes)	Fatality rate (per 100 high-risk damaged homes)
PH	175	10	4	2	2.3	40.0
MH–all types	156	43	19	12	12.2	44.2
DWMH	106	20	12	7	11.3	60.0
SWMH	50	23	7	5	14.0	30.4
All home types	331	53	23	14	6.9	43.4

unreinforced masonry stem walls with a crawl space. No positive attachment to the stem wall or interior piers was observed in these two PHs. Structurally, PHs constructed in this way—which is common across the Southeast—are similar to MHs in that they rely upon the weight of the home to resist uplift and, to an extent, sliding wind loads. While a PH will generally have a higher self-weight than a MH due to the larger structural member sizes used, any effects of this weight difference were not witnessed during the post-event damage assessment. Thus, it is apparent that the two PHs where fatalities transpired performed similar to MHs within the same region.

Based on the total number of homes observed with visible exterior damage, the tornado encompassed a fatality rate of seven fatalities per 100 homes for all housing types (Table 1). This fatality rate is nearly *seven times greater* than the fatality rate associated with the May 22, 2011 Joplin, Missouri, EF5 tornado where 80 residential fatalities occurred in 7,411 damaged homes (Kuligowski et al. 2014). The primary difference between these two disasters is the total number of MHs affected in each event. For instance, none of the 161 deaths in the Joplin, Missouri, tornado transpired in MHs (Kuligowski et al. 2014; Paul and Stimers 2012), and none or very few MHs were noted to have been impacted by the tornado. Yet, 19 of 23 fatalities in the Beauregard-Smith Station, Alabama, tornado were in MHs. As discussed prior, most homes in the Beauregard-Smith Station tornado failed closer to the base of the superstructure (e.g., wall-to-floor connection or anchoring system), subjecting the occupants to wind-blown debris and blunt-force trauma (Fig. 8). The fatality rate in MHs was 12 fatalities per 100 MHs damaged (11.3 and 14.0 for DWMHs and SWMHs). This fatality rate is 5.3 times higher compared to the number of fatalities per 100 PHs damaged in the Beauregard-Smith Station tornado.

Together, these findings illustrate that a primary cause of the high fatality rates in the Beauregard-Smith Station, Alabama, EF4 tornado was the elevated number of MHs, which provide minimal (with tie-down straps and ground anchor systems) or no (with alternative pan systems) positive anchoring to protect against wind-induced uplift forces that exceed the self-weight of the home. Each of the MH-tornado fatalities in Lee County also transpired in MHs built after 1983, suggesting that these structures were more susceptible to complete destruction compared to PHs despite being constructed under post-1976 HUD code construction standards. The mean age of MHs where fatalities occurred was 20 years old, where construction years ranged from 1983 to 2007. Fatality rates were similar across both MH types, with 12 of the 19 MH fatalities occurring in DWMH structures, compared to seven in SWMHs. Unfortunately, a common theme witnessed throughout the in-person damage survey was the lack of positive anchorage in both older site-built homes where fatalities occurred as well. This finding suggests that regardless of housing type and age, homes with no positive anchorage to resist uplift forces are at a much higher risk of incurring fatalities in violent tornadoes. Our hypothesis is that in a high wind event, these housing types sustain a structurally brittle failure (i.e., sudden, with little to no inelastic deformation prior to failure and thus little to no energy dissipation) at the foundation that prematurely compromises the integrity of the remaining structure and enhances the probability of occupants being killed or seriously injured. More detailed analysis of the tornado wind field is being conducted to evaluate at what wind speeds such destruction is likely, but the analysis is outside of the scope of this paper.

All Beauregard-Smith Station tornado fatalities occurred in the first 20 km of the damage path where the tornado lead time was approximately 9–12 min. The lack of fatalities in the remaining portions of the tornado path is likely due to the tornado weakening in intensity (resulting in fewer high-risk structural failures) in combination with the advanced warning from the NWS (i.e., tornado emergency warning) and the prior storm history that allowed those affected to better prepare for the tornado and seek shelter.

The portion of the tornado path where most (13 of 14 homes) fatalities were located was considered largely exurban land use density. And, as mentioned prior, the tornado did not strike any MH parks or communities. As discussed in Strader and Ashley (2018), nearly 80% of MHs in Alabama are not in MH parks, but rather exurban and rural land use. The more dispersed MH density makes it more likely that Alabama MHs are struck by a given tornado. Thus, the Beauregard-Smith Station, Alabama tornado is a prime example of the MH-tornado relationship that frequently plagues the Southeast US.

Conclusions

This study employed an interscience approach to investigate the March 3, 2019 Beauregard-Smith Station, Alabama, EF4 tornado event. The research encompassed two primary goals: (1) illustrate how Southeast US tornado disasters commonly unfold at the local scale and lead to fatalities due to the combination of a significant (EF2+) or violent (EF4+) tornado intersecting vulnerable MH residents; and (2) demonstrate how fine-scale built environment, LULC data, Doppler radar products, and rapid posttornado forensic assessments can be combined to better understand tornado impacts, specifically regarding fatalities. A bulleted list of conclusions is provided below:

- The Beauregard-Smith Station, Alabama, tornado is representative of tornado disasters in the Southeast US where the intersection of a significant or violent tornado with MH structures leads to a high number of fatalities despite impacting a relatively small number of buildings (e.g., Ashley 2007; Strader and Ashley 2018).
- Higher fatality rates were observed in MHs when compared to PHs. All (19 of 23) MH fatalities occurred in MHs built after 1983, and 15 of the 19 MH fatalities occurred in MHs built after 1994. Although this is just one tornado event, it provides further evidence that although all of these structures were built after the post-1976 HUD construction changes, and 75% after the 1994

HUD changes, they were still more vulnerable compared to PHs in the same region due to the minimal wind design requirements for homes located in HUD Wind Zone I.
- The fatality rate in the Beauregard-Smith Station, Alabama, tornado was seven times greater than that of the 2011 Joplin, Missouri, EF5 tornado. This greater fatality rate is at least in part attributed to the much larger percentage of MHs in the Beauregard-Smith Station, Alabama, tornado damage path compared to that of the Joplin, Missouri, tornado.
- All homes (MHs and PHs) where fatalities occurred and anchorage systems could be ascertained either entirely lacked positive anchorage to resist wind uplift forces beyond the self-weight of the home, or in the case of MHs with tie-down straps and ground anchors, had what minimal positive anchorage was present compromised by corrosion and other installation defects.

Ash et al. (2020) indicates that most MH residents in the Southeast US shelter inside their home during tornado events. Results from this study illustrate the potential consequences that come with this decision when a tornado strikes. Thus, although SPC and NWS forecast products in the days, hours, and minutes leading up to the event may have adequately communicated the tornado threat, the combination of MH residents sheltering in their homes and their housing structures failing at the base of the superstructure (i.e., ground anchoring) ultimately led to the high number of MH fatalities. Accordingly, this event seems to be an exemplar of the larger Southeast MH-tornado problem. While neither PHs or MHs are built to withstand violent tornado wind speeds (+166 mph), MHs observed in our study demonstrate a fatal flaw in that (1) anchorage is consistently the weakest link in the structural load path for HUD-compliant, Zone I MHs; and (2) anchorage failures in these MHs are often brittle due to either the complete lack of positive uplift resistance in pan anchorage systems, or compromised resistance in tie-down strap systems due to corrosion and improper installation. This mismatch between how MH residents expect their housing structures to perform and the compromised structural systems that exist creates a volatile and deadly scenario for a majority of MH residents in the Southeast US.

Southeastern US states that frequently experience fatal tornado events involving MHs (Strader and Ashley 2018) should consider implementing more stringent MH structural anchoring requirements for newly purchased and existing MHs. At the very least, results from this study should serve to initiate a dialogue among stakeholders, elected officials, emergency managers, and the public about the possibility of implementing programs or strategies aimed at improving MH structural resilience through the amendment of MH anchoring requirements. Currently, a large majority of MHs located in tornado-prone US regions such as Alabama, Mississippi, etc. are only required to comply with HUD Zone I standards. HUD Zone I standards require MHs to withstand a maximum wind speed of 70 mph (104 mph ASCE 7-16 equivalent). As such, MHs with the greatest odds of being struck by tornadoes often contain anchoring systems (e.g., the aforementioned pan system) that only resist horizontal or lateral wind forces from weak EF0 and EF1 tornadoes, while solely relying on the structure's own weight to resist any vertical or upward wind forces. As this study has illustrated, this type of anchoring promotes violent, unsafe failure sequences during significant (EF2+) tornado winds.

A potential solution for improving MH structural performance during tornado events is to require all MHs in tornado-prone regions to comply with HUD Zone II or III building and anchoring standards. Increasing anchoring requirements up to Zone II and III levels has been shown to improve MH performance during extreme winds (IBTS 2005; Simmons and Sutter 2008; Hebert and Levitan 2009). It is surmised that similar requirements for MHs in tornado-prone regions would also improve their structural performance and resilience during tornado events and reduce the odds of fatalities. Although this study does not directly assess or measure the mechanisms and economic costs for bringing all tornado-prone MHs up to Zone II or III requirements, our findings suggest that there is value in improving MH construction and anchoring standards when it comes to tornado impacts. Retrofitting and enforcing better anchoring systems for MHs would undoubtedly increase resident survivability and reduce future disaster costs.

As intentioned, a limitation of this study is that it focuses on one tornado disaster in the Southeast, and results should be extrapolated with care. Particularly with respect to the contrast in vulnerability between MHs and PHs, we recognize that the vulnerability of both housing types exists on a spectrum and characterizing their relative vulnerability in broad statements can overly simplify more nuanced issues. For example, our study has highlighted that there are some PHs that can perform similarly to MHs due to a complete lack of positive anchorage. Nevertheless, prior research (e.g., Ashley 2007; Sutter and Simmons 2010; Strader and Ashley 2018) has repeatedly demonstrated that the Southeast US does indeed suffer from a tornado-MH problem that leads to a disproportionate number of MH residents killed in tornado events. Results presented herein point to the need for future work aimed at targeted assessments of MH structural performance during tornado events. Additional research that includes more thoroughly investigating the relationships that exist among tornado wind speeds, structural response beyond structural design wind speeds, MH construction and anchorage installation practices (particularly the impacts of increased use of pan systems), fatalities, and survivability factors is also needed. Subsequent research by the authors will investigate and explore potential engineering mitigation strategies that may bolster MH resident safety during tornado events. Forthcoming research will also examine this issue from a cost-benefit standpoint so that recommendations to MH manufacturers, wholesale dealers, installers, and homeowners can be provided, reducing losses.

Findings and methodologies applied in this study should be used to further NWS Integrated Warning Teams' (i.e., forecasters, emergency manager, media partners, and engineers) and the general public's understanding of how tornado disasters take place. By improving tornado disaster knowledge, education, and assessment techniques, mitigation and resilience-building strategies can be developed and employed by local, state, and federal entities. Future consideration should be given to tornado events that intersect localized area of low-income populations where residents often live in MHs. Historically, the total financial cost on the underlying population and built environment for many of these Southeast tornado-MH events does not meet the minimum requirements for federal support or disaster recovery (Pacific Standard 2019). In addition, MH residents are less likely to have insurance to assist them in recovery (Talk Poverty 2019). These issues together exacerbate MH resident inequalities and result in long-lasting impacts to tornado disaster victims. In all, lines of communication should be opened between decision makers (e.g., FEMA, emergency managers, elected officials, policy makers) and members of the manufactured housing industry. These groups must work together to improve resident survivability and ensure the safety of MH residents not only in the Southeast US but in all tornado-prone regions throughout the country.

Data Availability Statement

Some data generated or used during the study are proprietary or confidential in nature and may only be provided with restrictions

(e.g., mobile/manufactured housing location data and the precise fatality data). All other data are made available upon request or are publicly available.

Acknowledgments

This research was supported by the National Oceanic and Atmospheric Administration (NOAA) Verifications of the Origins of Rotation Experiment in the Southeast (VORTEX-SE) Grant Nos. NA17OAR4590191 and NA19OAR4590213. Additional support was provided by the National Science Foundation under Award No. CMMI 18-41667, which formed the Structural Extreme Events Reconnaissance (StEER) network. Contributions from StEER and its members are acknowledged and appreciated, as well as Tim Marshall and Martin Montgomery, who also conducted on-site assessments and shared data and insights. Lastly, we would like to thank the anonymous reviewers for their thorough feedback, comments, and suggestions.

References

Ash, K. D. 2017. "A qualitative study of mobile home resident perspectives on tornadoes and tornado protective actions in South Carolina, USA." *GeoJournal* 82 (3): 533–552. https://doi.org/10.1007/s10708-016-9700-8.

Ash, K. D., M. J. Egnoto, S. M. Strader, W. S. Ashley, D. B. Roueche, K. E. Klockow-McClain, D. Caplen, and M. Dickerson. 2020. "Structural forces: Perception and vulnerability for tornado sheltering within mobile and manufactured housing in Alabama and Mississippi, USA." *Weather Clim. Soc.* 12 (3): 453–472. https://doi.org/10.1175/WCAS-D-19-0088.1.

Ashley, W. S. 2007. "Spatial and temporal analysis of tornado fatalities in the United States: 1880–2005." *Weather Forecasting* 22 (6): 1214–1228. https://doi.org/10.1175/2007WAF2007004.1.

Ashley, W. S., and S. M. Strader. 2016. "Recipe for disaster: How the dynamic ingredients of risk and exposure are changing the tornado disaster landscape." *Bull. Am. Meteorol. Soc.* 97 (5): 767–786. https://doi.org/10.1175/BAMS-D-15-00150.1.

Bodine, D. J., M. R. Kumjian, R. D. Palmer, P. L. Heinselman, and A. V. Ryzhkov. 2013. "Tornado damage estimation using polarimetric radar." *Weather Forecasting* 28 (1): 139–158. https://doi.org/10.1175/WAF-D-11-00158.1.

Brooks, H. E., and J. Correia Jr. 2018. "Long-term performance metrics for National Weather Service tornado warnings." *Weather Forecasting* 33 (6): 1501–1511. https://doi.org/10.1175/WAF-D-18-0120.1.

Burgess, D., et al. 2014. "20 May 2013 Moore, Oklahoma, tornado: Damage survey and analysis." *Weather Forecasting* 29 (5): 1229–1237. https://doi.org/10.1175/WAF-D-14-00039.1.

Census. 2020. "Explore census data." Accessed February 1, 2020. https://data.census.gov/cedsci/?q=mobile%20home.

Cutter, S. L., B. J. Boruff, and W. L. Shirley. 2012. "Social vulnerability to environmental hazards." In *Hazards vulnerability and environmental justice*, 143–160. Abingdon, UK: Routledge.

Egnew, A. C., D. B. Roueche, and D. O. Prevatt. 2018. "Linking building attributes and tornado vulnerability using a logistic regression model." *Nat. Hazard. Rev.* 19 (4): 04018017. https://doi.org/10.1061/(ASCE)NH.1527-6996.0000305.

FEMA. 2007. *February 2007 tornado recovery advisory: Understanding and improving performance of new manufactured homes during high-wind events*. FEMA DR 1679 RA5. Atlanta: FEMA.

FEMA. 2013. "Wind zone comparisons (HUD's MHCSS and FEMA 85)." Accessed March 3, 2020. https://www.fema.gov/media-library-data/20130726-1501-20490-5921/fema_p85_apndx_g.pdf.

Gibbs, J. G., and B. R. Bowers. 2019. "Techniques and thresholds of significance for using WSR-88D velocity data to anticipate significant tornadoes." *J. Oper. Meteorol.* 7 (9): 117–137. https://doi.org/10.15191/nwajom.2019.0709.

Hebert, K., and M. Levitan. 2009. "Performance of manufactured housing in Louisiana during Hurricanes Katrina and Rita." In *Proc., 11th American Conf. on Wind Engineering*. San Juan, PR: American Association of Wind Engineering, Polytechnic Institute of Puerto Rico.

HIFLD (Homeland Infrastructure Foundation-Level Data). 2020. "HIFLD open data." Accessed January 17, 2020. https://hifld-geoplatform.opendata.arcgis.com/.

IBTS (Institute for Building Technology and Safety). 2005. *An assessment of damage to manufactured homes caused by Hurricane Charley*. Prepared for the US Department of Housing and Urban Development. Washington, DC: Office of Policy Development and Research.

Kensler, C. D. 1985. "The Morgan Hill earthquake of April 24, 1984—Effects on mobile homes." *Earthquake Spectra* 1 (3): 607–613. https://doi.org/10.1193/1.1585281.

Kijewski-Correa, T., D. Prevatt, K. Mosalam, I. Robertson, and D. Roueche. 2018. "Structural Extreme Events Reconnaissance (StEER) network." Accessed February 22, 2020. https://www.steer.network/.

Kingfield, D. M., and J. G. LaDue. 2015. "The relationship between automated low-level velocity calculations from the WSR-88D and maximum tornado intensity determined from damage surveys." *Weather Forecasting* 30 (5): 1125–1139. https://doi.org/10.1175/WAF-D-14-00096.1.

Kuligowski, E. D., F. T. Lombardo, L. T. Phan, M. L. Levitan, and D. P. Jorgensen. 2014. *Final report, National Institute of Standards and Technology (NIST) technical investigation of the May 22, 2011, tornado in Joplin, Missouri*. Rep. No. National Construction Safety Team Act Reports (NIST NCSTAR)-3. Gaithersburg, MD: National Institute and Standards.

Lombardo, F. T., D. B. Roueche, and D. O. Prevatt. 2015. "Comparison of two methods of near-surface wind speed estimation in the 22 May 2011 Joplin, Missouri Tornado." *J. Wind Eng. Ind. Aerodyn.* 138 (Mar): 87–97. https://doi.org/10.1016/j.jweia.2014.12.007.

Marshall, T. P. 1993. "Lessons learned from analyzing tornado damage." . *In The Tornado: Its structure, dynamics, prediction, and hazards*, edited by C. Church, D. Burgess, C. Doswell, and R. Davies-Jone. Hoboken, NJ: Wiley. https://doi.org/10.1029/GM079p0495.

Marshall, T. P. 2002. "Tornado damage survey at Moore, Oklahoma." *Weather Forecasting* 17 (3): 582–598. https://doi.org/10.1175/1520-0434(2002)017<0582:TDSAMO>2.0.CO;2.

McDonald, J. R., and K. C. Mehta. 2004. "A recommendation for an enhanced Fujita scale (EF-Scale)." Accessed January 6, 2020. https://www.spc.noaa.gov/faq/tornado/ef-ttu.pdf.

Microsoft US Building Footprints. 2018. "Building footprints." Accessed January 12, 2020. https://www.microsoft.com/en-us/maps/building-footprints.

NCEI (National Centers for Environmental Information). 2019. "Billion-dollar weather and climate disasters: Summary stats." Accessed January 5, 2020. https://www.ncdc.noaa.gov/billions/summary-stats.

NSSL (National Severe Storms Laboratory). 2019. "Multi-radar/multi-sensor system MRMS." Accessed February 14, 2020. https://www.nssl.noaa.gov/projects/mrms/.

NWS and BMX (National Weather Service and Birmingham, AL). 2019. "Beauregard-Smiths station EF-4 tornado (Macon/Lee counties)." Accessed March 3, 2019. https://www.weather.gov/bmx/event_03032019beauregard.

NWS (National Weather Service) and KMXX Doppler Radar Site. 2019. "East Alabama radar." Accessed October 30, 2020. https://radar.weather.gov/ridge/radar.php?rid=mxx&product=N0R&overlay=11101111&loop=no.

Pacific Standard. 2019. "After the storm: Why mobile home owners continue to suffer more from tornado damage." Accessed March 15, 2020. https://psmag.com/social-justice/tornadoes-put-mobile-home-owners-at-severe-risk.

Paul, B. K., and M. Stimers. 2012. "Exploring probable reasons for record fatalities: The case of 2011 Joplin, Missouri, tornado." *Nat. Hazards* 64 (2): 1511–1526. https://doi.org/10.1007/s11069-012-0313-3.

Prevatt, D. O., W. Coulbourne, A. J. Graettinger, S. Pei, R. Gupta, and D. Grau. 2012a. *Joplin, Missouri, Tornado of May 22, 2011: Structural damage survey and case for tornado-resilient building codes*. Reston, VA: ASCE.

Prevatt, D. O., J. W. van de Lindt, E. W. Back, A. J. Graettinger, S. Pei, W. Coulbourne, R. Gupta, D. James, and D. Agdas. 2012b. "Making the case for improved structural design: Tornado outbreaks of 2011." *Leadersh. Manage. Eng.* 12 (4): 254–270. https://doi.org/10.1061/(ASCE)LM.1943-5630.0000192.

Rhee, D. M., and F. T. Lombardo. 2018. "Improved near-surface wind speed characterization using damage patterns." *J. Wind Eng. Ind. Aerodyn.* 180 (Sep): 288–297. https://doi.org/10.1016/j.jweia.2018.07.017.

Roueche, D., T. Kijewski-Correa, D. Prevatt, B. Davis, K. Mosalam, I. Robertson, K. Turner, C. Hodges, and B. Rittelmeyer. 2019. *January 2019 tornadoes in the southeastern US: Field assessment team early access reconnaissance report EARR*. Austin, TX: DesignSafe-CI. https://doi.org/10.17603/ds2-eb6e-tr31.

Roueche, D. B., F. T. Lombardo, and D. O. Prevatt. 2017. "Empirical approach to evaluating the tornado fragility of residential structures." *J. Struct. Eng.* 143 (9): 04017123. https://doi.org/10.1061/(ASCE)ST.1943-541X.0001854.

Roueche, D. B., and D. O. Prevatt. 2013. "Residential damage patterns following the 2011 Tuscaloosa, AL and Joplin, MO tornadoes." *J. Disaster Res.* 8 (6): 1061–1067. https://doi.org/10.20965/jdr.2013.p1061.

Rumbach, A., E. Sullivan, and C. Makarewicz. 2020. "Mobile home parks and disasters: Understanding risk to the third housing type in the United States." *Nat. Hazard. Rev.* 21 (2): 05020001. https://doi.org/10.1061/(ASCE)NH.1527-6996.0000357.

Simmons, K. M., and D. Sutter. 2008. "Manufactured home building regulations and the February 2, 2007 Florida tornadoes." *Nat. Hazards* 46 (3): 415–425. https://doi.org/10.1007/s11069-007-9192-4.

Smith, B. T., R. L. Thompson, A. R. Dean, and P. T. Marsh. 2015. "Diagnosing the conditional probability of tornado damage rating using environmental and radar attributes." *Weather Forecasting* 30 (4): 914–932. https://doi.org/10.1175/WAF-D-14-00122.1.

Sparks, P. R. 1985. *Building damage in South Carolina caused by the tornadoes of March 28, 1984*. Rep. No. CETS-CND-031. Washington, DC: National Academies.

Strader, S. M., W. Ashley, A. Irizarry, and S. Hall. 2014. "A climatology of tornado intensity assessments." *Meteorol. Appl.* 22 (3): 513–524. https://doi.org/10.1002/met.1482.

Strader, S. M., and W. S. Ashley. 2018. "Finescale assessment of mobile home tornado vulnerability in the central and southeast United States." *Weather Clim. Soc.* 10 (4): 797–812. https://doi.org/10.1175/WCAS-D-18-0060.1.

Sutter, D., and K. M. Simmons. 2010. "Tornado fatalities and mobile homes in the United States." *Nat. Hazards* 53 (1): 125–137. https://doi.org/10.1007/s11069-009-9416-x.

Talk Poverty. 2019. "A record-breaking tornado season is pummeling mobile home residents." Accessed December 14, 2020. https://talkpoverty.org/2019/07/30/tornadoes-mobile-homes-south/.

Theobald, D. M. 2005. "Landscape patterns of exurban growth in the USA from 1980 to 2020." *Ecol. Soc.* 10 (1): 32. https://doi.org/10.5751/ES-01390-100132.

Thompson, R. L., B. T. Smith, J. S. Grams, A. R. Dean, J. C. Picca, A. E. Cohen, E. M. Leitman, A. M. Gleason, and P. T. Marsh. 2017. "Tornado damage rating probabilities derived from WSR-88D data." *Weather Forecasting* 32 (4): 1509–1528. https://doi.org/10.1175/WAF-D-17-0004.1.

Van Den Broeke, M. S., and S. T. Jauernic. 2014. "Spatial and temporal characteristics of polarimetric tornadic debris signatures." *J. Appl. Meteorol. Climatol.* 53 (10): 2217–2231. https://doi.org/10.1175/JAMC-D-14-0094.1.

Vickery, P. J., P. F. Skerlj, J. Lin, L. A. Twisdale Jr., M. A. Young, and F. M. Lavelle. 2006. "HAZUS-MH hurricane model methodology. II: Damage and loss estimation." *Nat. Hazard. Rev.* 7 (2): 94–103. https://doi.org/10.1061/(ASCE)1527-6988(2006)7:2(94).

Wickham, J., C. Homer, J. Vogelmann, A. McKerrow, R. Mueller, N. Herold, and J. Coulston. 2014. "The multi-resolution land characteristics (MRLC) consortium—20 years of development and integration of USA national land cover data." *Remote Sens.* 6 (8): 7424–7441. https://doi.org/10.3390/rs6087424.